Original Manuscript

SCIENCE PROGRESS

Science Progress
2022, Vol. 105(2) 1–25

DOI: 10.1177/00368504221102742
journals.sagepub.com/home/sci

Fatigue life prediction of brake discs for high-speed trains via thermal stress

Jiao Luo, Jiazhi Liu, Ziyun You and Xintian Liu
School of Mechanical and Automotive Engineering, Shanghai University of Engineering Science, Shanghai, China

Abstract
As one of the essential components of the braking system, the high-speed train brake disc is an integral part of ensuring the safety of the train. The main objective of this study is to conduct thermal analysis and reliable life prediction on brake discs. The research was conducted by developing a programmer spectrum of brake discs with high-speed train brake discs. According to the results of numerical analysis and the S-N curve of the material, the temperature distribution on the surface of the brake disc is determined, and the fatigue life of the brake disc is predicted. The comparison with the service life of the brake disc verifies the rationality of the calculation results. In addition, a fatigue damage probability model of brake discs is established based on the theory of fatigue cumulative damage. Through the relationship between the reliability of mechanical parts and the number of load cycles, the reliable life of the brake disc under different working conditions is predicted. This work establishes a method of reliable life analysis for brake discs of high-speed trains based on the load spectrum, which could analyze the life and reliability of brake discs more systematically.

Keywords
Thermal stress, road load spectrum, fatigue damage probabilistic model, reliable life ; high-speed train brake discs

Introduction

The brake disc's fatigue life may be anticipated using the collected load during train operation in conjunction with the fatigue-related mechanism or S-N curve. As a result, to precisely anticipate the brake disc's fatigue life, it is important to examine the load signals obtained. There are several mature research approaches for handling load signals.

Corresponding author:
Xintian Liu, School of Mechanical and Automotive Engineering, Shanghai University of Engineering Science, Shanghai, China.
Email: xintianster@gmail.com

The service life of high-speed train brake discs is related to the ambient temperature, braking pressure, and random load from the track.[1] When the train is braking, the brake disc temperature rises rapidly due to the braking force. Due to the different heat dissipation effects of each part of the brake disc, there is a temperature gradient in the brake disc, which provides conditions for the generation of thermal stress. Thermal stress could easily cause thermal fatigue of the brake disc and accelerate the formation of cracks inside the brake disc.[2] In addition, brake disc surface temperature is also related to the brake disc material. The brake disc is usually made of cast steel or forged steel. Due to the limitation of casting level, the qualified rate of cast steel brake disc is low, and defects are prone to appear in the casting process. Generally, the brake discs of high-speed trains are mostly made of forged steel. Forged steel shows good mechanical properties at high temperatures, ensuring the processing quality of brake discs. Jin et al. 2016[3] studied the change of material parameters of train brake disc with temperature, which provided methods for brake disc design and process improvement.

Wang et al. 2009[4] analyze the temperature distribution on the surface of the brake disc, and the numerical solution is usually needed. A simulation tool could be used to analyze the temperature field and stress field of the brake disc. Guo et al. 2016[5] used the differential quadrature method to solve the temperature distribution along the radial direction of three different materials of brake discs. They found that the temperature distribution along the radial direction of materials with good thermal conductivity usually presented uniform distribution. Que et al. 2019[6] analyzed the stress field of a forged steel brake disc and verified that a forged steel brake disc could meet the requirements of safe braking. Wang et al. 2008[7] conducted numerical analysis on the braking process of the high-speed train, and the theoretical results were consistent with bench test results. Zhang et al. 2011[8] found that the highest temperature exists on the friction surface through simulation analysis. The convective heat transfer coefficient was obtained by Yang et al. 2008[9] through CFD (Computational Fluid Dynamics) numerical simulation, which did not need to rely on the traditional theory for calculation.

Belhocine et al.[10–12] calculated the temperature change of brake disc surface during train braking and related numerical calculation. The heat source of the brake disc could be analyzed based on the change of heat source. The process of friction heat generation of brake disc was studied, and the change of mechanical properties of brake disc material after temperature rise was obtained.[13,14]

The mechanism of mechanical stress formation in the brake disc was studied by Chen et al. 2021.[15] Wang et al. 2019[16] analyzed how continuous thermal and mechanical stresses affect crack extension and microstructural evolution in brake discs. Li et al. 2015[17] conducted thermal cycling tests to simulate the temperature change during braking, and the volume change of the steel caused by microstructural transformation was considered in the numerical simulation. Sawczuk et al. 2018[18] presented the results of several years of investigations on the railway disc brake under varying wear conditions in relation to the UIC (International Union of Railways) requirements for brake pad approval. Besides, Yan et al. 2015[19] used numerical simulations to systematically compare the thermofluid properties of cross-drilled ventilated brake discs with standard and included radial vanes. The heat transfer enhancement mechanism of the cross-drilled hole is elucidated. Li et al. 2021[20] discussed the current research status and development trend of automotive disc brake materials.

Bench tests are usually used for brake discs of high-speed trains to collect load signals during driving. Due to the limitations of the test conditions and the inevitable signal interference, the collected brake disc load signals generally contain interference signals such as noise and abnormal values. Therefore, it is necessary to preprocess the original signals, such as wavelet threshold denoising.[21,22] According to the principle of load analysis, the amplitude, mean value, extreme value, and standard deviation of load signals could reflect the overall characteristics of load signals.[23–25] For the preprocessed signals, extracting the average load amplitude is usually necessary. The commonly used method is the rain flow counting method, which is widely used to extract the load amplitude of mechanical structures and vehicle parts.[26,27] In order to reflect the train driving conditions more honestly, it is often necessary to extrapolate the collected load signals. Commonly used extrapolation methods include over threshold extrapolation, parameter extrapolation, and extrapolation by mileage or quantile.[28] It is necessary to compile the program spectrum.[29] Liu et al. 2017,[30] Liu et al. 2022[31,32] described the compilation process of load spectrum in detail and studied the life of relevant parts through load spectrum.

Therefore, considering the service condition of the brake disc, it is necessary to carry out a thermal analysis. The main content of this work is as follows. Firstly, a load spectrum is constructed from the collected brake disc load signals. Secondly, the thermal fatigue analysis of the brake disc is carried out. Next, the reliability of the brake disc is analyzed. Based on the collected load spectrum, a reliable life analysis method of high-speed train brake discs is proposed, which could analyze the life and reliability of brake discs more systematically.

Load signals analysis of the brake disc

The research process of this paper is shown in Figure 1.

As an important part of the braking system, the load form and material of the brake disc will affect the braking efficiency. Therefore, a high-reliability level of the brake disc is the premise to ensure the safe operation of the train.[33]

The driving conditions of the high-speed train could be roughly divided into three stages: accelerating process at a lower speed, approximately driving at a uniform speed and decelerating process. Generally, the train also experiences a similar acceleration and deceleration process when passing through a station. Section 2 mainly studies the load on the brake disc during the deceleration process of the train.

Load signals preprocessing

In engineering, to save workforce and material resources, a braking test is usually carried out on the test bench.[34] Acceleration signals collected by the sensor device are shown in Figure 2. Due to the inevitable interference of environmental factors, the collected acceleration signals contain some abnormal values. These inevitable abnormal signals will affect the compilation of the acceleration spectrum and even affect the accuracy of the service life prediction with the brake disc. Therefore, it is necessary to preprocess the original load signals.

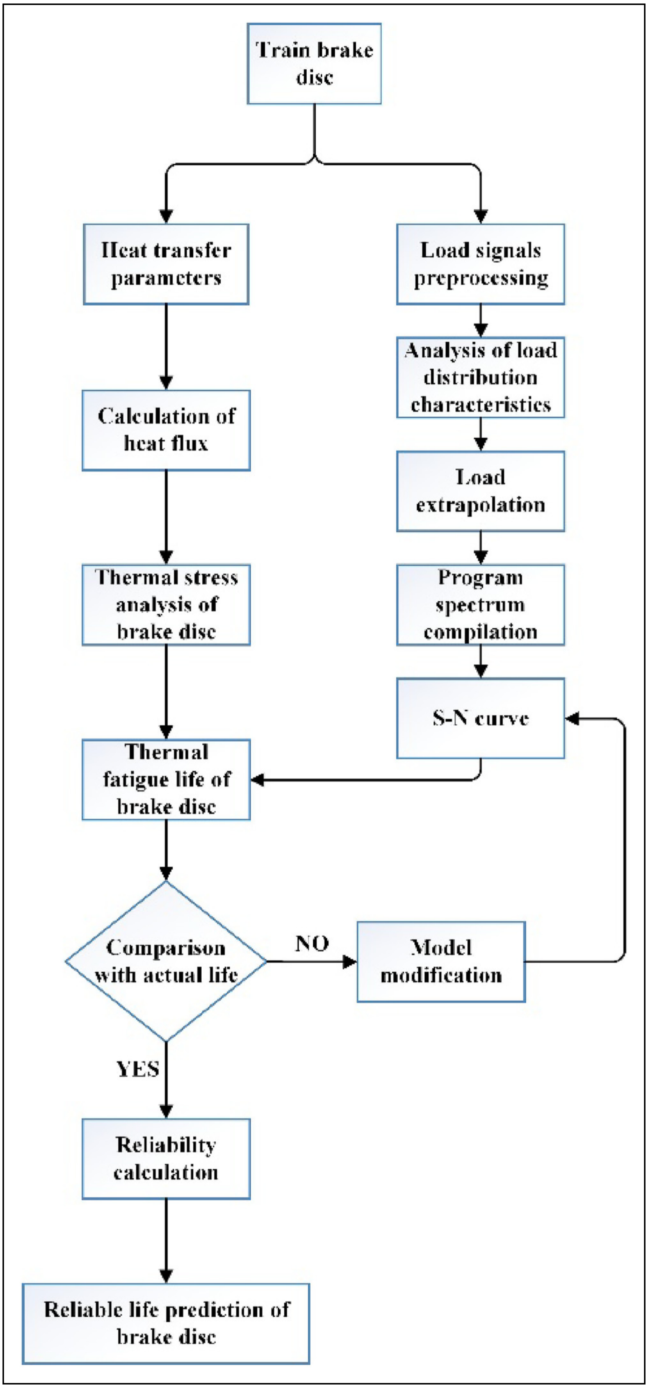

Figure 1. Flow chart of brake disc fatigue life.

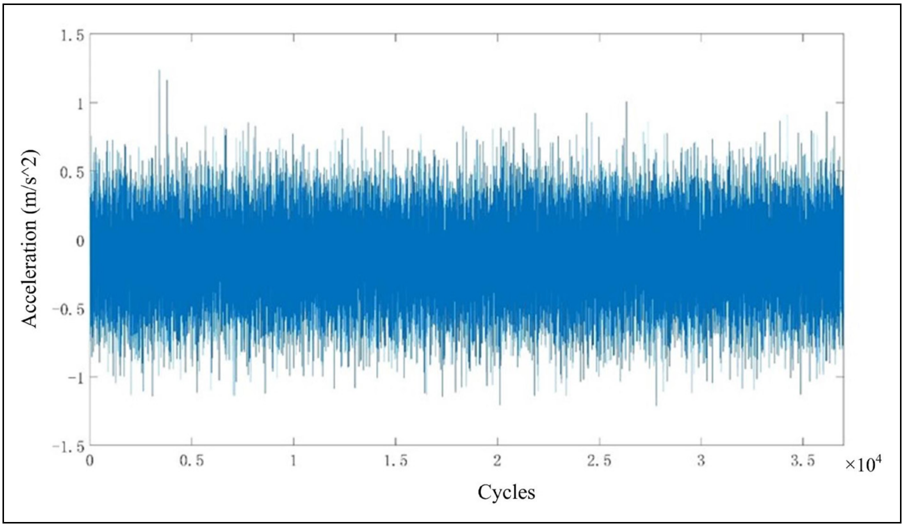

Figure 2. Acceleration of train during braking.

Due to the interference of the service environment, some unavoidable abnormal loads will appear in collected signals. These abnormal signals will have a great impact on fatigue life prediction. To predict the service life of the brake disc accurately, it is necessary to eliminate them. This paper uses a 3σ criterion to deal with outliers.[35,36]

For a group of test data, the mean value and standard deviation could be obtained from equations (1) and (2).

$$\overline{X} = \frac{1}{n}\sum_{i=1}^{n} X_i \tag{1}$$

$$\sigma = \sqrt{\frac{1}{n-1}\sum_{i=1}^{n}(X_i - \overline{X})^2} \tag{2}$$

$$|X_i - \overline{X}| > k\sigma \tag{3}$$

where k is a constant. According to 3σ criterion, k is taken as 3.

If the signal value conforms to equation (3), it is judged as an abnormal value. Otherwise, it is regarded as a normal value for subsequent processing.

Due to the noise of collected signals, interference will be produced when the load spectrum is processed. Therefore, to obtain the ideal load signals, it is necessary to remove the noise signals. For signal de-noising, the threshold method could be used to separate noise and useful signals. The threshold method has a better denoising effect and can further improve the signal-to-noise ratio of the signal. Threshold processing generally includes two parts: threshold and threshold function.

The threshold function could quantize the wavelet coefficients. There are two common thresholding methods: Hard thresholding and Soft thresholding. Both methods have their limitations: the hard threshold function has discontinuities in some areas, while the soft threshold function has deviations. Therefore, we could reset the function domain to obtain a better processing effect. According to the above analysis, signal processing toolboxes are used to complete the load signals preprocessing. Select the appropriate number of decomposition layers for the load signals following outlier elimination; a comparison of load signals is presented in Figure 3.

It could be seen from Figure 3 that the denoising process is mainly to remove outliers and oscillation signals. After denoising, the load signals present a gentler trend. The above work lays a foundation for the extraction of load average amplitude.

Analysis of load distribution characteristics

The initial speed of train braking is 250 km/h, and the average amplitude of load signals of the brake disc could be extracted after preprocessing. The amplitude could reflect the overall characteristics of load signals, and it could be used to program the load spectrum and predict the fatigue life of structural components. Before extracting the amplitude of load signals, the loads should be counted. In mechanical fatigue, load counting transforms the load-time history into a regular load cycle process. The two-parameter method could better reflect the overall characteristics of the load. This study uses the rain flow counting method to extract the mean and amplitude.[37]

Before further analyzing the distribution characteristics of load signals, extracting the amplitude, and counting the frequency of collected load signals,[38] the rain flow counting

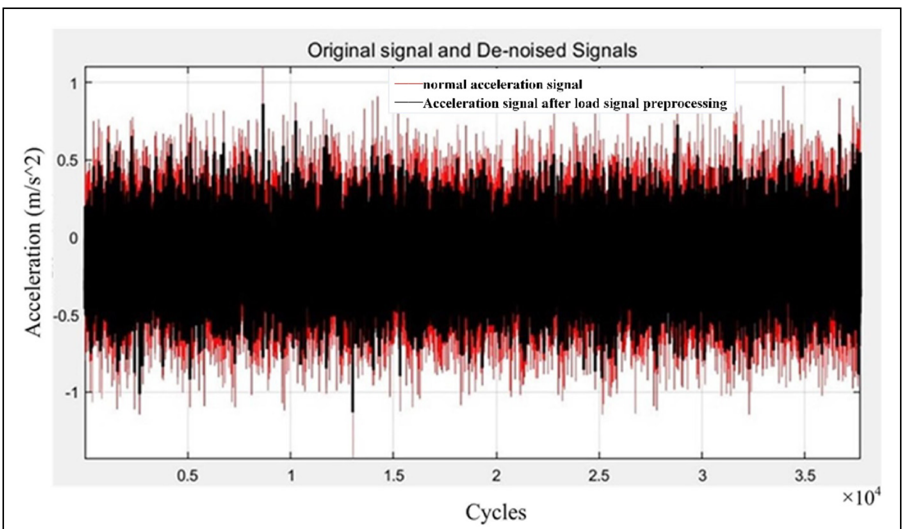

Figure 3. Original signal and De-noised signals.

method is used to extract the load cycles, and their mean and amplitude are counted. The counting results are shown in Figures 4 and 5.

In Figures 4 and 5, the load is braking force, converting the acceleration of the train into braking force is for subsequent stress analysis.

It could be seen from Figure 4 that the mean frequency distribution is peak-symmetrical, and the distribution function part could conform to the t-location-scale distribution, logical distribution and normal distribution. As shown in Figure 5, the amplitude-frequency distribution is a unimodal distribution, and its distribution may conform to the Weibull distribution, lognormal distribution and gamma distribution. Therefore, the probability distribution density function with unimodal characteristics is used to fit the mean and amplitude of load signals.

The distribution model is obtained by fitting the probability density function according to the load signals distribution in Figures 4 and 5, which could more intuitively reflect load distribution characteristics. The common probability distribution models include exponential distribution, normal distribution, gamma distribution, Weibull distribution and lognormal distribution. The expressions of several common probability distribution density functions are shown in Table 1.

Different probability density functions are used to fit the frequency statistical histogram to obtain the probability distribution functions. In addition, log likelihood estimation is used to fit the functions. The fitting results are shown in Figures 6 and 7, and log likelihood estimation results are shown in Tables 2 and 3.

As shown in Figure 6, the t-Location-scale, logistic, and normal distribution all fit better to the mean. They can be tested using the log-likelihood estimation method to determine the best fit. The log-likelihood estimates are shown in Table 2. In the log-likelihood estimation test, a larger estimate indicates a better fit. In Table 2, the estimated value of the normal distribution is the largest among several distribution models, and the normal distribution is the best fit compared with the other two distribution models.

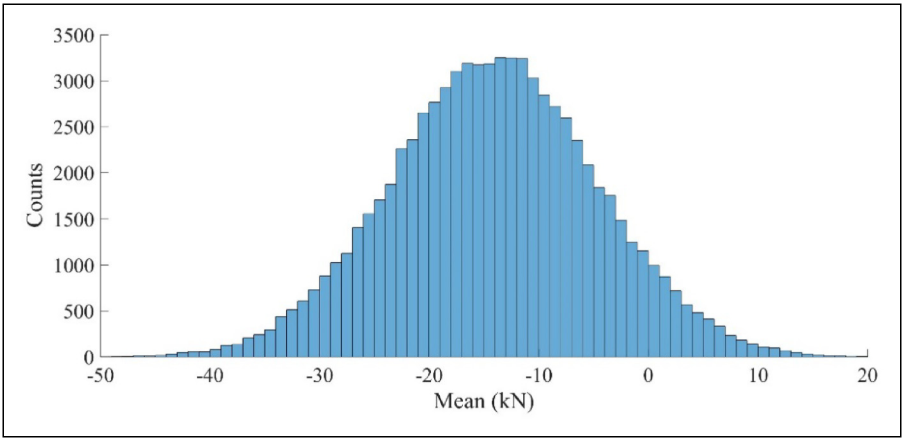

Figure 4. Statistical histogram of mean frequency.

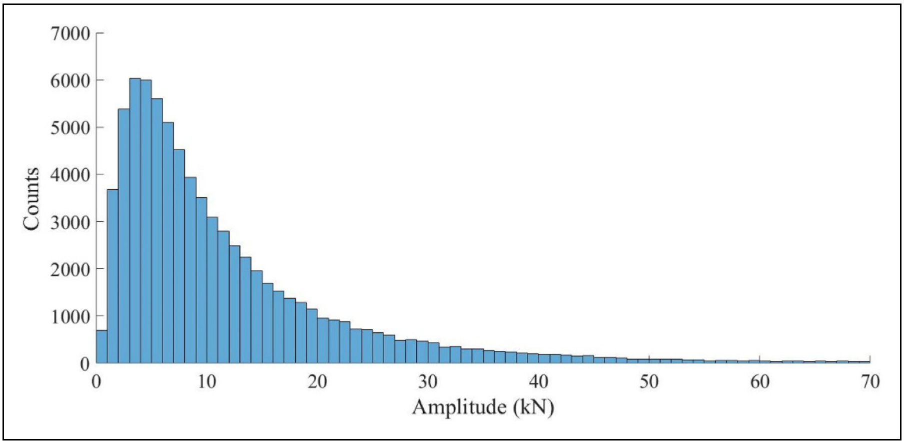

Figure 5. Statistical histogram of amplitude frequency.

Table 1. One-dimensional distribution ndensity function.

Distribution model	Probability density function $f(x)$
Exponential distribution	$f(x) = \lambda e^{-\lambda x}$
Normal distribution	$f(x) = \frac{1}{\sqrt{2\pi}\sigma} e^{-\frac{(x-u)^2}{2\sigma^2}}$
Gamma distribution	$f(x, \beta, \alpha) = \frac{\beta^{\alpha}}{\Gamma(\alpha)} x^{\alpha-1} e^{-\beta x}, x > 0$
Weibull distribution	$f(x\,\lambda\,k) = \frac{k}{\lambda} \left(\frac{x}{\lambda}\right)^{k-1} e^{-(x/\lambda)^k}, \ x > 0$
Log-normal distribution	$f(x, \mu, \sigma) = \frac{1}{\sqrt{2\pi}\sigma} e^{-\frac{(\ln x-u)^2}{2\sigma^2}}, \ x > 0$

The probability density function of normal distribution is shown in equation (4)

$$f(x) = \frac{1}{\sqrt{2\pi}\sigma} e^{\frac{-(x-\mu)^2}{2\sigma^2}}, \ -\infty < x < +\infty \tag{4}$$

where x is a random variable, μ is a position parameter, and σ is a scale parameter. According to the fitting results, the mean and amplitude of the function are substituted into equation (4), and the probability density function of load mean distribution is obtained as shown in equation (5).

$$f(x) = \frac{1}{9.43\sqrt{2\pi}} e^{\frac{-(x+14.04)^2}{177.85}} \tag{5}$$

As shown in Figure 7, for the load amplitude, the fitting effect of the lognormal distribution is better. The log-likelihood estimation values are shown in Table 3. In statistical theory, the larger the log-likelihood estimate, the better the fitting effect. Therefore, the lognormal distribution is the most suitable for the load amplitude.

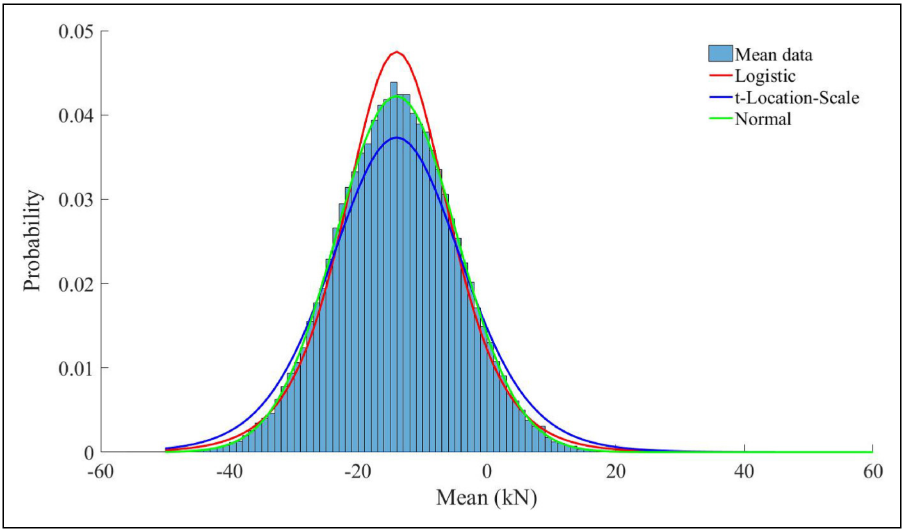

Figure 6. Mean fitting.

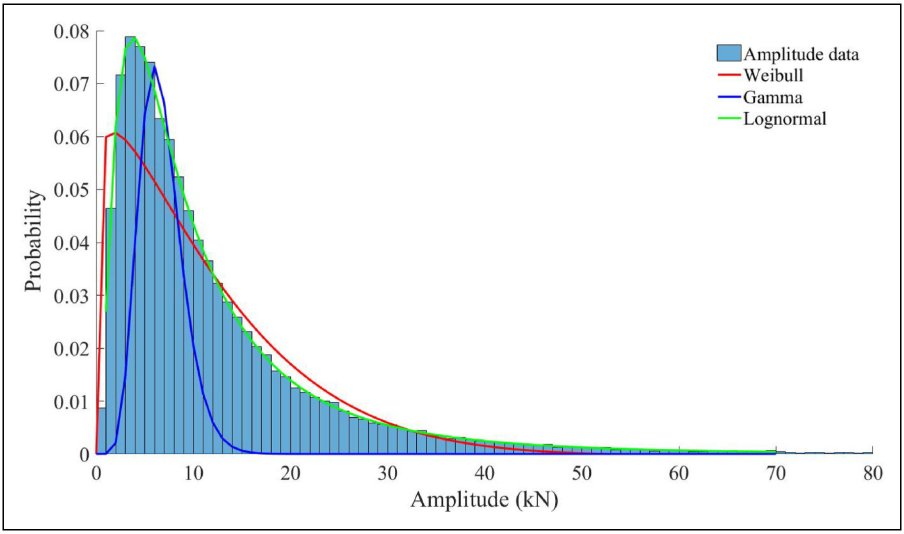

Figure 7. Amplitude fitting.

According to equation (6), the probability density function of lognormal distribution could be expressed as follows

$$f(x) = \frac{1}{\sqrt{2\pi}\sigma} e^{\frac{-(\ln x-\mu)^2}{2\sigma^2}}, x > 0 \tag{6}$$

Table 2. Log likelihood estimation test of mean under different mathematic models.

Mathematic model	Log likelihood estimation	(μ, σ)
t-Location-Scale	−282701	(14.04, 9.42)
Logistic	−282797	(14.04, 5.40)
Normal	−282045	(14.04, 9.43)

Table 3. Log likelihood estimation test of amplitude under different mathematic models.

Mathematic model	Log likelihood estimation
Weibull	−271656
Gamma	−270277
Lognormal	−265502

According to the fitting results, the probability density function of load amplitude distribution is obtained by substituting parameter's value, as shown in equation (7)

$$f(x) = \frac{1}{0.9\sqrt{2\pi}} e^{\frac{-(\ln x - 2.13)^2}{1.62}} \tag{7}$$

Load extrapolation

The data collected in the bench test is data for a period or under certain conditions, while the actual working condition of the train is long-distance operation. Therefore, to predict the fatigue life of the brake disc more reasonably, it is necessary to extrapolate the collected load signals. Due to the stable running state of the train during driving, this section uses the parameter method combined with the mileage to extrapolate the load signals.[1] According to the statistical point of view, 10^6 cycles could represent the real load condition, and the load signals are extrapolated to 10^6 cycles. The load signals are extrapolated by using the methods, as shown in equation (8)

$$N_c = k_m N_m \tag{8}$$

Among them, N_c is the number of loads after extrapolation, $m = 12{,}3$ which respectively represents conditions of train acceleration, uniform speed and deceleration. N_m is the accumulated times of load signals under different working conditions, k_m is the expansion coefficient ($k_m = 10^6/N$), and N is the total accumulated times of load signals under actual conditions.

Program spectrum compilation

Due to the load signals obtained could not be directly applied to the fatigue life prediction, it is necessary to compile the collected load signals into the program load spectrum. The program spectrum is equivalent to loading loads of different amplitudes in a certain order, which is more in line with the working conditions of the mechanical structure in service.[39] Generally, a one-dimensional 8-level load could better reflect the overall characteristics of load signals. In this paper, the fatigue life of the brake disc is predicted by compiling a one-dimensional 8-level program load spectrum.

To reflect the overall characteristics of the load signals more accurately, this study uses the amplitude scale coefficient to divide collected load signals into unequal intervals.[40] In the process of compiling the load spectrum, the commonly used amplitude scale factor is shown in Table 4.

One dimensional load program spectrum is compiled by load amplitude and its corresponding frequency. The amplitude ratio coefficient method is used to divide the amplitude and compile the 8-level load spectrum of the brake disc. The division of the amplitude interval is shown in equation (9).

$$\begin{cases} l_0 = A_{\min},\ \ l_8 = A_{\max} \\ l_i = l_{i-1} + \dfrac{A_{\max} + A_{\min}}{\sum_{i=1}^{8} k_i} k_i \end{cases} \tag{9}$$

where $A_{\max},\ A_{\min}$ are the maximum and minimum values of load amplitude, $l,\ l_{i-1}$ are the upper and lower limits of i amplitude range, and k_i is the proportional coefficient of amplitude range.

$$n_i = N_c \int_{l_{i-1}}^{l_i} f_A \mathrm{d}x \tag{10}$$

where n_i is the i load frequency corresponding to the level amplitude, N_c is the extrapolated load frequency and f_A is the probability density function of load amplitude.

According to the program spectrum construction method shown in equation (9) and equation (10), the one-dimensional program load spectrum shown in Table 5 could be obtained.

Thermal stress analysis of the brake disc

In the braking process of high-speed trains, the purpose of deceleration is achieved through the surface friction between the friction plate and brake disc. Due to the uneven heat dissipation on the surface of the brake disc, there is a temperature gradient inside the brake disc, which leads to the generation of thermal stress. Relevant literature research showed that the influence of thermal stress on the service life of high-speed train brake disc is far greater than the random load caused by road vibration.[41–43] Therefore, based on the thermodynamic theory, the temperature distribution on the surface of the brake disc is obtained by numerical analysis. At the same time, the fatigue life of the

Table 4. Amplitude scale factor.

Load level i	1	2	3	4	5	6	7	8
Scale factor k_i	1	0.90	0.85	0.725	0.575	0.425	0.275	0.125

Table 5. Braking load program spectrum.

Load level	Amplitude (kN)	Frequency(Hz)
1	7.319	37716
2	18.245	14980
3	28.309	5957
4	37.367	2223
5	44.843	871
6	50.594	370
7	54.620	161
8	56.92	59

brake disc is calculated according to the material parameters of the brake disc and the S-N curve of 25Cr2MoV steel.

Heat transfer parameters

Heat transfer usually occurs between two objects with temperature differences. The phenomenon of heat transfer will last for a period until the temperature difference between objects disappears. There are three common ways of heat transfer: heat conduction, heat convection and heat radiation.[44]

(1) If there is a temperature difference inside an object or between several close objects, heat will be transferred from high temperature to low temperature. In this case, the heat conduction law is shown in equation (11).

$$q = -k_e \frac{\mathrm{d}T}{\mathrm{d}x} \tag{11}$$

In equation (12), q is heat flux (w/m^2), k_e represents thermal conductivity, and $\frac{\mathrm{d}T}{\mathrm{d}x}$ is temperature gradient (K/m).

(2) Thermal convection usually occurs on the surface of solid and liquid in contact. Thermal convection could be divided into natural convection and forced convection. The convective heat could be described by equation (12).

$$q = H(T_b - T_z) \tag{12}$$

where H is the convective heat transfer coefficient (w/m^{2}K), T_b represents the surface temperature of the solid and T_z is the fluid temperature (°C).

(3) Generally, when an object radiates energy outward, it will also absorb the energy radiated by other objects. The net heat transfer between objects could be calculated by Stefan Boltzmann equation.

$$q = \kappa\beta A_1 F_{12}(T_1^4 - T_2^4) \tag{13}$$

$\kappa$is emissivity, usually taken as 0.8. β is Stefan Boltzmann constant, usually taken as 5.67×10^{-8}W / (m$^2 \cdot$ K^4). A_1 is the area of radiation surface 1, F_{12} is the shape coefficient between radiation surface 1 and radiation surface 2. T_1 represents the absolute temperature of radiation surface 1, and T_2 represents the ambient temperature.

(4) In the braking process, the coefficient of the fluid heat transfer system will change with the train speed, fluid motion state and fluid properties. If the convective heat transfer coefficient is expressed by H, the expression is

$$H = \frac{N_u L}{\lambda} \tag{14}$$

Among them, $N_u = 0.337 \times R_e^{0.8} P_r^{0.35}$, called Nusselt number. L is the characteristic length of the brake disc (m), where λ is taken as the thermal conductivity of the air (W/ (m·K)). P_r is the Prandtl number of the air, the value is about 0.7. R_e is the Reynolds number of the fluid, $R_e = \rho v L/\mu$, where ρ (kg/m^3), v (m/s) and μ (Pa·s) are the density, velocity and viscosity coefficient of the fluid. Therefore, the convective heat transfer coefficient H could be expressed as follows

$$H = \frac{0.377 \times (\rho v L / \mu)^{0.8} P_r^{0.35} L}{\lambda} \tag{15}$$

It could be seen from equation (15) that the convection heat transfer coefficient is related to the fluid velocity. The velocity of the fluid is related to the speed of the vehicle, so it is necessary to analyze the law of the fluid convection heat transfer coefficient with the speed. The relationship between the convective heat transfer coefficient and the speed is shown in Figure 8.

It could be seen from Figure 8 that when the train speed decreases, the convective heat transfer coefficient also decreases. When the running speed is lower than 50 km/h, the change rate is larger. The increase in H-factor leads to an increase in thermal stress and a decrease in fatigue life.

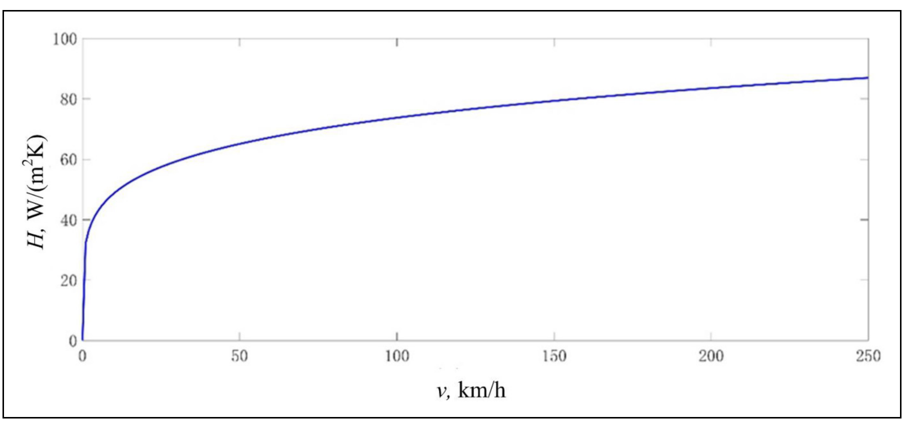

Figure 8. Relationship between convective heat transfer coefficient and vehicle speed.

Calculation of heat flux

If kinetic energy in the braking process is converted into heat energy, there is

$$Q_t = \frac{1}{2}mv_0^2 - \frac{1}{2}mv_t^2 \tag{16}$$

where m is the mass of the train body, v_0 is the initial braking speed and v_t is running speed at time t. Q_t is heat energy generated from time t_0 to time t.

The heat generation rate is obtained by deriving equation (17).

$$P_t = \frac{dQ_t}{dt} = -ma(v_0 + at) \tag{17}$$

where a is acceleration during braking. During the braking process of the train, about 80% of heat will remain in the brake disc,[6] and the heat flux of the brake disc is

$$q = \eta \frac{P_t}{n' S_f} \tag{18}$$

where energy transfer coefficient $\eta = 0.8$, n' is the number of friction surfaces on each axle. $S_f = \pi(R_1^2 - R_2^2)$, S_f is the swept area of the friction plate, R_1 is the outer diameter of the brake disc and R_2 is the inner diameter of the brake disc.

According to the brake disc size, train braking acceleration and other relevant parameters, as shown in Table 6.

According to the data in Table 6, the change of heat flux during train braking is shown in Figure 9.

It could be seen from Figure 9 that during train braking, the heat flux first decreases from a higher level and then increases slowly. When the train starts braking, the braking pressure exerted by the braking system is large. When the vehicle speed decreases, a small braking force is applied to ensure the safe operation of the train. Moreover, the heat generation is reduced, which is conducive to improving the service life of the brake disc.

Thermal stress analysis of the brake disc

There are two sources of stress on the brake disc: one is the thermal stress caused by the temperature gradient inside the brake disc. The other is the inertia force and braking pressure from the brake disc, as well as the random load brought by the track. According to relevant research, the internal thermal stress of the brake disc is much greater than that of

Table 6. Heat flux at speed of 250 km/h.

Braking time t (s)	Heat flux (W/m^2)
0~12	$q = 1116.3 \times (250 - 0.2t)$
13~30	$q = 223.3 \times (154 - 0.04(t\text{-}12))$
31~42	$q = 613.9 \times (125 - 0.11(t - 30))$
43~54	$q = 1060.5 \times (83 - 0.19(t - 42))$

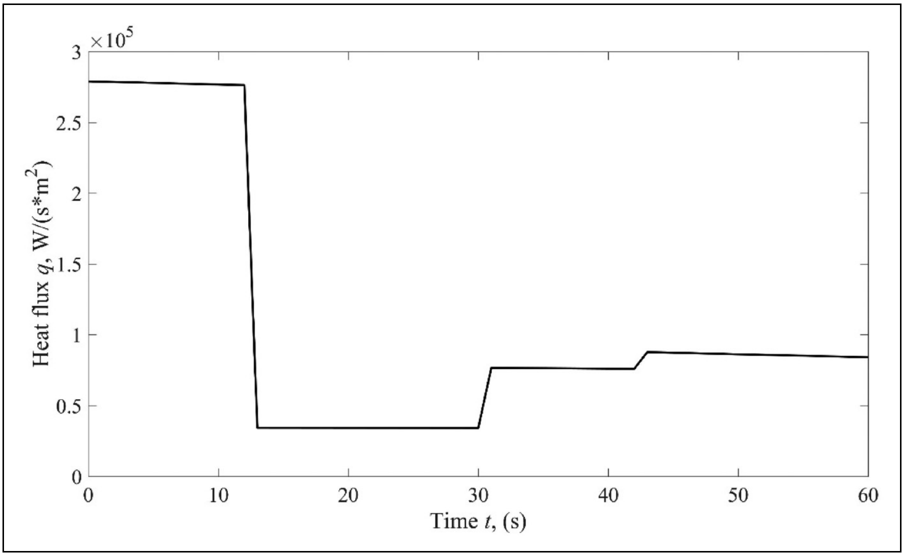

Figure 9. Heat flux variation of the brake disc.

Table 7. Brake disc size parameters.

Outer diameter of brake disc (mm)	Inner diameter of brake disc (mm)	Thickness (mm)	Average friction radius (mm)
640	258	40	247

the wheel rail and external environment.[7] Therefore, for the stress analysis of the brake disc, mainly considers the influence of thermal stress on the fatigue life of the brake disc.

The brake disc material studied in this paper is 25Cr2MoV, and the dimension parameters of the brake disc are shown in Table 7.[44]

The material parameters of 25Cr2MoV are shown in Table 8.[43]

To study the temperature distribution on the surface of the brake disc, presents thermal sensors in bench tests may be used to acquire the temperature distribution on the surface of the brake disc. Then, the commonly applied numerical analysis approach is employed to investigate the brake disc's surface temperature distribution.

Some assumptions are made to perform numerical analysis.

1. The brake disc is in full contact with the friction plate;
2. The braking pressure acting on the friction plate is evenly distributed;
3. The wear of brake disc and friction plate is not considered;

This paper uses Abaqus 2020 software for numerical modeling and analysis. The surface temperature distribution of the brake disc could be obtained as shown in Figure 10.

Table 8. Physical property parameters of 25Cr2MoV steel.

Density (kg/m^3)	7.62×10^3		Melting point (°C)		1400	
Physical property	Temperature (°C)					
	25	100	200	300	400	500
Elastic modulus E (GPa)	211	208	203	197	188	178
Poisson's ratio μ	0.3	0.3	0.31	0.31	0.32	0.32
Thermal conductivity λ (W/(m•K))	32.0	32.4	32.9	31.8	29.7	28.2
Specific heat capacity c (J/(kg•K))	519	519	519	523	523	523
Coefficient of linear expansion α (10^{-6}J/K)	11.6	12.6	12.9	13.2	13.7	14.0

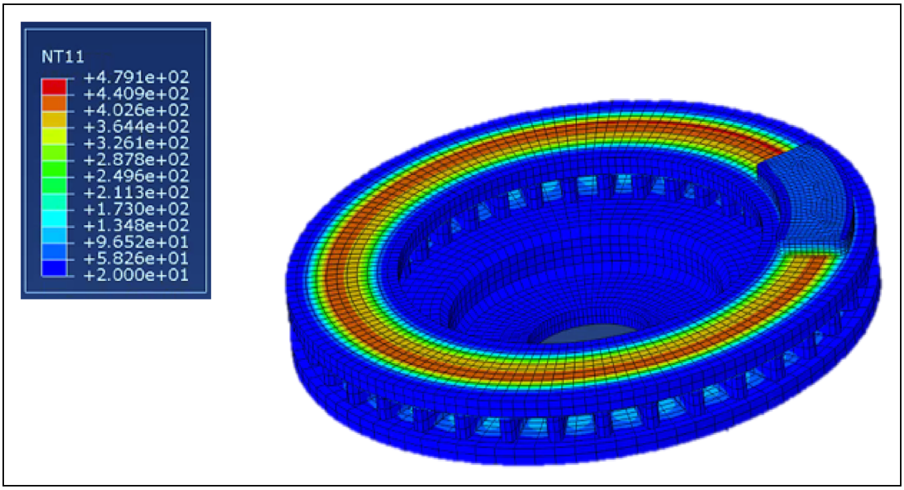

Figure 10. Surface temperature distribution of brake disc.

For the brake disc studied in this paper, the initial speed of train braking is 250 km/ h and the initial temperature in the braking process is close to room temperature. The result in Figure 11 is the time at which the temperature difference reaches its maximum or the time at which the larger braking force is converted to a smaller braking force. It could be seen from Figure 10 that there are temperature gradients in different radius directions, which is the cause of thermal stress. Under the average friction radius, the maximum temperature is 479.1 °C. Along the radial direction of the brake disc, the temperature value shows a downward trend.

To analyze the fatigue performance of the brake disc under high temperatures more accurately, it is necessary to analyze the mechanical parameters of the brake disc material. The conventional mechanical properties and chemical composition of 25Cr2MoV are shown in Tables 9 and 10.[45]

At different temperatures, the material parameters of the brake disc will change. The tensile strength and yield strength of forged steel change obviously with temperature, as shown in Figure 11.[37]

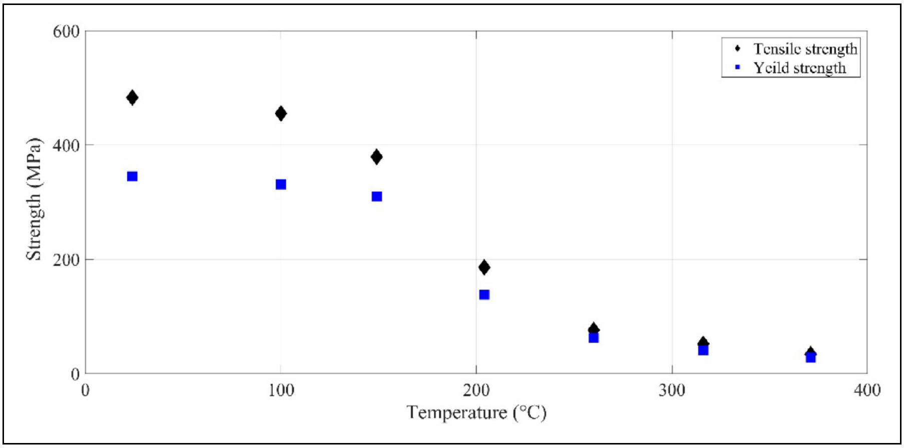

Figure 11. Fatigue strength of forged steel at different temperatures.

Table 9. Chemical composition of 25Cr2MoV steel.

Element	C	Si	Mn	P	S	Ni	Cr	Mo	V	Cu
Contents	0.27	0.25	0.51	0.01	0.01	0.08	1.70	0.30	0.21	0.10

Table 10. Conventional mechanical properties of 25Cr2MoV.

σ_s(MPa)	σ_b(MPa)	δ_5(%)	ψ(%)	E (GPa)	HB
1090	1042	18	63	211	308

It could be seen from Figure 11 that the fatigue strength of forged steel is greatly affected by temperature. When the temperature is lower than 200°C or higher than 400°C, the tensile strength and yield strength of forged steel decrease obviously with the increase of temperature. The decrease of the fatigue strength of the brake disc material will lead to plastic deformation inside the brake disc, which has a great influence on the service life of the brake disc. Therefore, it is necessary to study the temperature distribution of the brake disc in the braking process.

Thermal fatigue life of the brake disc

Through Basquin equation:

$$\sigma_a = \sigma_f N_f^b \tag{19}$$

The S-N curve of material could be obtained. And fatigue life of forged steel structures under different stress levels could be calculated. Where σ_a is stress amplitude, b is fatigue strength index.

$$\sigma_f = (1 + \psi)\sigma_{\mathrm{b}} \tag{20}$$

ψ is percent reduction of area, and σ_f is fatigue strengthening coefficient.

The S-N curve of 25Cr2MoV material is shown in Figure 12.[37]

The regular operation of the brake disc is an important guarantee for the safe operation of the train. The existence of thermal stress accelerates the internal plastic deformation of the brake disc and accelerates the fatigue failure process of the brake disc. Therefore, to ensure the safety of train operation, it is necessary to analyze the service life of the brake disc. The load studied is mainly thermal stress. According to the brake disc material's S-N curve, combined with the brake disc model's numerical analysis, the number of cycles that the brake disc could withstand at different temperatures is obtained, as shown in Table 11.

It could be seen from Table 11 that the equivalent thermal stress is $\sigma_{T_{eqv}} = 641$ MPa. Which is substituted into S-N curve of 25Cr2MoV material, and the number of failure cycles is 107684. Assuming that the train brakes 50 times a day and 360 days a year, the service life of the brake disc made of this material is about 5.98 years. The average service life of a forged steel brake disc is about 5.06 years,[46] which shows that the calculation result is reasonable.

Reliability analysis of the brake disc

In the design and production process of structure, it is necessary to analyze the reliability of products.[47,48] Therefore, it is necessary to analyze the reliability of a high-speed brake disc. Based on the reliability theory, considering the influence of thermal stress on the fatigue life of the brake disc, a fatigue damage probabilistic model is established. On this basis, the service life of brake discs with different reliability is calculated.

Fatigue damage probabilistic model

From the perspective of probability and statistics, it is generally considered that the functional failure of structures or components is a random event. If the event A represents that component could work normally and the event B represents the component fails, the probability space of the component could be expressed by equation (21)

$$\Omega = (A, B) \tag{21}$$

According to the reliability theory, the reliability of structure could be expressed by equation (22)

$$R = P(A) = 1 - P(B) \tag{22}$$

The load and dimension parameters of the brake disc are usually randomly distributed. Therefore, combines the probability and statistics model with fatigue cumulative damage theory to establish the probabilistic model of brake disc fatigue damage. If U is used to represent fatigue strength of component and D is used to represent cumulative fatigue damage, the critical failure condition of components could be expressed as

$$U = D \tag{23}$$

It could be seen that the reliability of parts is

$$R = P(U > D) \tag{24}$$

According to the fatigue cumulative damage theory, there is a certain relationship between each stress level and the number of load cycles under the corresponding stress level

$$\sigma_1^s N_1 = \sigma_2^s N_2 = \cdots = \sigma_k^s N_k = M \tag{25}$$

It could be obtained from equation (26)

$$N_k = \frac{M}{\sigma_k^s} \tag{26}$$

where N_k and σ_k represent theoretical fatigue life and stress amplitude under k-level cyclic load respectively. M is a constant and s is the slope of S-N curve of material in logarithmic coordinates.

According to the linear fatigue damage theory, if

$$\sum_{k=1}^{j} \frac{n_k}{N_k} = 1 \tag{27}$$

the parts were regarded as failed. n_k is the actual action times under k-level load. It could

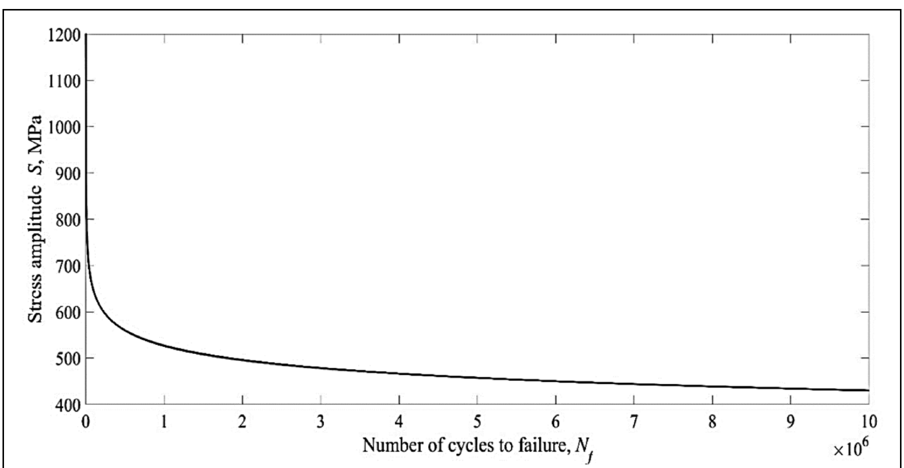

Figure 12. S-N curve of material 25Cr2MoV.

Table 11. Thermal stress at different temperatures.

Temperature (°C)	Thermal stress (MPa)	Amount of damage
479.1	1144	6.7×10^{-3}
440.9	1084	3.6×10^{-3}
402.6	986	1.2×10^{-3}
364.4	886	3.7×10^{-4}
326.1	796	1.1×10^{-4}
287.8	697	2.4×10^{-5}
249.6	598	4.2×10^{-6}
211.3	501	5.6×10^{-7}
173.0	401	4.5×10^{-8}
134.8	299	1.6×10^{-9}
96.5	202	1.9×10^{-11}
58.3	101	7.0×10^{-15}

be obtained by substituting N_k in the equation (25).

$$\sum \sigma_k^s n_k = M \tag{28}$$

$$\sum \sigma_i^s \cdot n_i = \sigma_i^s \cdot N_i \tag{29}$$

Reliable life prediction of the brake disc

If the component fails under k-level stress σ_k after N_k cycles, fatigue strength U is shown in equation (31)

$$U = \sigma_k^s N_k \tag{31}$$

According to the program spectrum, several values of U could be obtained. According to equation (32) to (34), the probability distribution parameters of U could be obtained.[49]

$$s = \frac{-\sum_{i=1}^{n}(d_i - d)(g_i - g)}{\sum_{i=1}^{n}(d_i - d)^2} \tag{32}$$

$$\mu_{Ln(U)} = d \cdot s + g \tag{33}$$

$$\sigma_{Ln(U)} = \sqrt{\frac{1}{n}\sum_{i=1}^{n}(g_i + d_i s - \mu_{Ln(U)})^2} \tag{34}$$

where, $d_i = Ln(\sigma_{ik}),\ g_i = Ln(N_{ik}),\ d = \frac{1}{n}\sum_{i=1}^{n} d_i,\ g = \frac{1}{n}\sum_{i=1}^{n} g_i$.

Assuming that the fatigue damage strength U satisfies lognormal distribution, assumed $\Phi(x) \sim N(0, 1)$. Reliability of brake disc could be expressed as

$$R_d = P(Ln(U) - Ln(D)) = \Phi\left(\frac{\mu_{Ln(U)} - Ln(D)}{\sigma_{Ln(U)}}\right) \tag{35}$$

Table 12. Fatigue life of brake disc under different reliabilities.

Reliabilities	Cycles	Years
99%	60345	3.35
95%	73706	4.09
50%	121521	6.75

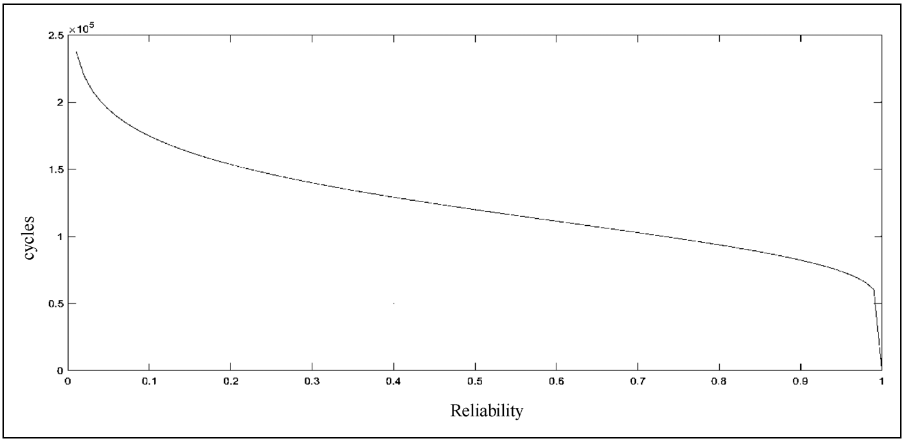

Figure 13. Fatigue life of brake disc under different reliabilities.

It is necessary to analyze the failure situation under different working conditions to ensure the safety of train operation. Therefore, we need to transform equation (36) into the following.

$$Ln(D) = \mu_{Ln(U)} + \sigma_{Ln(U)}\Phi^{-1}(1 - R) \tag{37}$$

The cumulative fatigue damage D is

$$D = \exp[\mu_{Ln(U)} + \sigma_{Ln(U)}\Phi^{-1}(1 - R)] \tag{38}$$

If the fatigue life of the brake disc under a certain reliability is N_R, it could be expressed as

$$N_R = \frac{\exp[\mu_{Ln(U)} + \sigma_{Ln(U)}\Phi^{-1}(1 - R)]}{\sum P_i \times \sigma_i^s} \tag{39}$$

where P_i is the ratio of loading times of the structural member under i-level stress σ_i to the total loading times.

The obtained thermal stress is substituted into equation (38). Assuming that the train brakes 50 times a day and a year is regarded as 360 days, the fatigue life of the brake disc under different reliability could be obtained, as shown in Table 12 and Figure 13.

It could be seen from Table 12 that the calculated theoretical service life of a brake disc is 3.35 years while $R = 99\%$. Under this reliability, the reliability of the brake disc is very high and fatigue failure will not occur generally. If $R = 95\%$, the theoretical service life of the brake disc is 4.09 years. It could be seen that the reliability level of the brake disc with this reliability is high, and fatigue failure is not easy to occur. To ensure the service quality of the brake disc, the service condition of the brake disc could be checked regularly. If $R = 50\%$, the theoretical service life of the brake disc is 6.75 years. The reliability of the brake disc under this reliability is low, and fatigue failure is can occur easily. Therefore, to ensure the safe operation of the train, the brake disc should be replaced in time and should not be used anymore.

Conclusions

The purpose of this study is to present a reliable life analysis method for high-speed train brake discs based on the collected load spectrum, which could be used to analyze the life and dependability of brake discs more systematically. The following summarises the paper's primary contents.

1. The frequency statistics of average amplitude and the probability distribution density function are used to fit the distribution features of the acquired load signals. The parameter and mileage methods are used to extrapolate the load signals, and the probability distribution density function is used to assemble the one-dimensional program spectrum.
2. A three-dimensional model of the brake disc is created using the geometric parameters of the brake disc. Through thermodynamic theory and the application of boundary conditions, a numerical model of the brake disc is built, and the brake disc's surface temperature distribution is determined. Equivalent thermal stress is determined based on the numerical analysis results, laying the groundwork for reliable brake disc life prediction. The fatigue life of the brake disc is determined using the S-N curve of the brake disc material. The calculated results are verified by comparing them to the actual service life of forged steel brake discs.
3. The fatigue damage probabilistic model of the brake disc is created using reliable life analysis methods and fatigue cumulative damage theory. The fatigue life of brake discs under various reliability conditions is predicted by considering the effect of thermal stress.

Author contributions

Conceptualization and methodology were performed by Jiao Luo and Jiazhi Liu, data curation was performed by Ziyun You, supervision was performed by Liu Xintian, reviewing and editing were performed by Jiazhi Liu. The first draft of the manuscript was written by Jiao Luo, and all authors commented on previous versions of the manuscript. All authors read and approved the final manuscript.

Data availability statement

Data sharing is not applicable to this article as no new data were created or analyzed in this study.

Declaration of conflicting interests

The author(s) declared no potential conflicts of interest with respect to the research, authorship, and/or publication of this article.

Funding

The author(s) received no financial support for the research, authorship, and/or publication of this article.

ORCID iDs

Xintian Liu https://orcid.org/0000-0002-3395-9176

References

1. Li JS, Lin HT, Li HP, et al. Simulation analysis of temperature field of alloy forged steel brake disc for high speed train. *Journal of the China Railway Society* 2006; 28: 45–48.
2. Jiang L, Jiang YL, Liang YU, et al. Thermal analysis for brake disks of SiC/6061 al alloy co-continuous composite for CRH3 during emergency braking considering airflow cooling. *Transactions of Nonferrous Metals Society of China* 2012; 22: 2783–2791.
3. Jin WW, Wang CC, Fang MG, et al. Thermal sensitivity analysis of material parameters of brake discs for high-speed trains. *Railway Locomotives and Rolling Stock* 2016; 36: 22–23.
4. Wang XD and Chen H. Numerical simulation of temperature field and thermal stress field of high-speed train brake discs. *Railway Vehicles* 2009; 47: 5–6.
5. Guo J, Wang ZM and Yao XS. Modeling and analysis of the temperature field of high-speed train brake discs. *Chinese Journal of Applied Mechanics* 2016; 33: 407–413.
6. Que HB, Qian KC and Jin WW. Simulation analysis of temperature and thermal stress of high-speed train brake discs. *Locomotive and Rolling Stock Technology* 2019; 4: 9–11.
7. Wang Y, Chen H and Li M. Numerical simulation of the braking process of high-speed train brake discs. *Mechanics* 2008; 35: 15–17.
8. Zhang T, Wang MX, Ding YQ, et al. Coupling analysis of the temperature field and thermal stress field of the brake disc of a motor vehicle. *Journal of Lanzhou Jiaotong University* 2011; 30: 119–122.
9. Yang Y. *Research on thermal fatigue evaluation method of SiCp/A356 composite brake disc for high-speed train*. Beijing: Beijing Jiaotong University; 2008.
10. Belhocine A and Bouchetara M. Thermal analysis of a solid brake disc. *Appl Therm Eng* 2012; 32: 59–67.
11. Ghadimi B, Kowsary F and Khorami M. Thermal analysis of locomotive wheel-mounted brake disc. *Appl Therm Eng* 2013; 51: 948–952.
12. Bauzin JG and Laraqi N. Three-dimensional analytical calculation of the temperature in a brake disc of a high-speed train. *Appl Therm Eng* 2019; 154: 668–675.
13. Ghazaly NM, Belhocine A, Cho CD, et al. Thermal analysis of both ventilated and full disc brake rotors with frictional heat generation. *Applied & Computational Mechanics* 2014; 8: 31–44.
14. Dhir DK. Thermo-mechanical performance of automotive disc brakes. *Materials Today Proceedings* 2018; 5: 1864−1871.

15. Chen A and Kienhöfer F. The failure prediction of a brake disc due to nonthermal or mechanical stresses. *Eng Fail Anal* 2021; 124: 105319.
16. Wang Z, Han J, Domblesky JP, et al. Crack propagation and microstructural transformation on the friction surface of a high-speed railway brake disc. *Wear* 2019; 428–429: 45–54.
17. Li Z, Han J, Yang Z, et al. Analyzing the mechanisms of thermal fatigue and phase change of steel used in brake discs. *Eng Fail Anal* 2015; 57: 202–218.
18. Sawczuk W. Analytical model coefficient of friction (COF) of rail disc brake on the basis of multi-phase stationary tests. *Mainteance and Reliability* 2018; 20: 57–67.
19. Yan HB, Feng SS, Yang XH, et al. Role of cross-drilled holes in enhanced cooling of ventilated brake discs. *Appl Therm Eng* 2015; 91: 318–333.
20. Li W, Yang X, Wang S, et al. Research and prospect of ceramics for automotive disc-brake. *Ceram Int* 2021; 47: 10442–10463.
21. Li W, Liu ZS and Ge YJ. Several methods of wavelet denoising. *Journal of Hefei University of Technology* 2002; 25: 167–172.
22. Yu JW, Qian CL, Zheng SL, et al. Study on optimization processing method of vehicle measured load spectrum based on wavelet transform theory. *Automot Eng* 2020; 42: 965–971.
23. Wang ML, Liu XT, Wang XL, et al. Fatigue test analysis of automotive key parts based on censored data and small sample setting. *Qual Reliab Eng Int* 2017; 33: 1031–1043.
24. Bi JH, Chen HL and Ren HP. Fatigue life analysis of contact wire based on rain flow counting method. *Acta Sinica* 2012; 34: 34–39.
25. Zhu SP, Liu Q, Lei Q, et al. Probabilistic fatigue life prediction and reliability assessment of a high-pressure turbine disc considering load variations. *Int J Damage Mech* 2018; 27: 1569–1588.
26. Li SS, Liu XT, Wang X, et al. Fatigue life prediction for automobile stabilizer bar. *International Journal of Structural Integrity* 2019; 11: 303–323.
27. Liu XT, Zhang MH, Wang HJ, et al. Fatigue life analysis of automotive key parts based on improved peak-over-threshold method. *Fatigue & Fracture of Engineering Materials & Structures* 2020; 43: 1824–1836.
28. Liu XT, Qi HZ, Wang XL, et al. Reliability analysis and evaluation of differential system based on low load strengthening model. *Qual Reliab Eng Int* 2016; 32: 647–662.
29. Dong GJ, Han J, Yan F, et al. Study on accelerated editing method of load spectrum for fatigue analysis of auto parts. *China Mech Eng* 2020; 31: 543–552.
30. Liu XT, Zheng SL, Chen T, et al. Durability life prediction of a reducer system based on low-amplitude load strengthening and damage. *J Chin Soc Mech Eng* 2017; 38: 81–91.
31. Liu XT, Liu JZ, Wang HJ, et al. Prediction and evaluation of fatigue life considering material parameters distribution characteristic. *International Journal of Structural Integrity* 2022; 13: 309–326. Doi: 10.1108/IJSI-11-2021-0118.
32. Liu XT, Wu Q, Su SC, et al. Evaluation and prediction of material fatigue characteristics under impact loads: review and prospects. *International Journal of Structural Integrity* 2022; 13: 251–277. Doi: 10.1108/IJSI-10-2021-0112.
33. Xu JM, Zhang HQ, Chen Q, et al. Safety assessment and life prediction model of fast train brake discs. *J Tsinghua Univ* 2006; 46: 609–612.
34. Wahlstrom J, Soderberg A, Olander L, et al. A disc brake test stand for measurement of airborne wear particles. *Lubr Sci* 2009; 21: 241–252.
35. Wang ML, Liu XT, Wang XL, et al. Research on load spectrum construction of automobile key parts based on monte carlo sampling. *J Test Eval* 2018; 46: 1099–1110.
36. Geng SL, Liu XT, Yang XB, et al. Load spectrum for automotive wheels hub based on mixed probability distribution model. *Proceedings of the IMechE, Part D: Journal of Automobile Engineering* 2019; 233: 3707−3720.

37. Schijve J. *Fatigue of structures and materials*. Beijing: Aviation Industry Press; 2014.
38. Wang SC, Liu XT, Jiang CJ, et al. Prediction and evaluation of fatigue life for mechanical components considering anelasticity-based load spectrum. *Fatigue & Fracture of Engineering Materials & Structures* 2021; 44: 129–140.
39. Zhang YS, Wang GQ, Wang JX, et al. Compilation method for load spectrum of engineering vehicle drive train. *Trans Chin Soc Agric Eng* 2011; 27: 179–183.
40. Luo ZJ and Zuo JY. Conjugate heat transfer study on a ventilated disc of high-speed trains during braking. *J Mech Sci Technol* 2014; 28: 1887–1897.
41. Wang Z, Han J, Liu X, et al. Temperature evolution of the train brake disc during high-speed braking. *Advances in Mechanical Engineering* 2019; 11: 1–10.
42. Zhang Y, Jin X, He M, et al. The convective heat transfer characteristics on outside surface of vehicle brake disc. *Int J Therm Sci* 2017; 120: 366–376.
43. Wang ZB, Xiang XW, He WK, et al. *Mechanical engineering material performance data manual*. Beijing: Mechanical Industry Press; 1995.
44. Haddad WM. Thermodynamics: the unique universal science. *Entropy* 2017; 19: 621.
45. Chen H, Qiao X, Zheng JJ, et al. Analysis on the fracture of 25Cr2MoV high temperature fastening bolts. *Mongolia Electric Power Technology* 2018; 36: 50–52.
46. Wu SC, Zhang SQ and Xu ZW. Thermal crack growth-based fatigue life prediction due to braking for a high-speed railway brake disc. *Int J Fatigue* 2016; 87: 359–369.
47. Zhu SP, Liu Q, Zhou J, et al. Fatigue reliability assessment of turbine discs under multi-source uncertainties. *Fatigue & Fracture of Engineering Materials & Structures* 2018; 41: 1291–1305.
48. Mao K, Liu XT, Li SS, et al. Reliability analysis for mechanical parts considering hidden cost via modified quality loss model. *Qual Reliab Eng Int* 2021; 37: 1373–1395.
49. Liu TY. Fatigue reliability analysis of structures under multi-stage constant amplitude loading proceedings of the third global Chinese aviation science and technology symposium. Chinese Aeronautical Society of China. 2005.

Author biographies

Jiao Luo is currently working as a lecturer of Mechanical engineering at Shanghai University of Engineering Science since 2010. Her research area is focused on fatigue life prediction and reliability design theory.

Jiazhi Liu is pursuing his Master's degree at Shanghai University of Engineering Science. His research area is focused on fatigue life prediction and reliability design theory.

Ziyun You received his Master's degree in vehicle engineering from Shanghai University of Engineering Science (China) in 2021. His research area is focused on fatigue life prediction and reliability design theory.

Xintian Liu is currently working as an associate professor of vehicle engineering at Shanghai University of Engineering Science (China) since 2007. His research area is focused on product quality control, fatigue life prediction and evaluation, uncertainty of mechanical system, reliability design theory and vehicle system dynamics.